Proceedings of the 8th World Congress on Civil, Structural, and Environmental Engineering (CSEE'23)
Lisbon, Portugal – March 29 – 31, 2023
Paper No. ICSECT 147
DOI: 10.11159/icsect23.147

Reaction Kinetic Studies of the Electrical Conductivity in Dissolution Experiments for the Identification of Alkali-Reactive Aggregate

Hartmut Gyde[1], Schmidt-Döhl Frank[1], Püstow Anna[1]
[1]Institute of Materials, Physics and Chemistry of Buildings Hamburg University of Technology
Eißendorfer Straße 42, 21073 Hamburg, Germany
Gyde.hartmut@tuhh.de; Schmidt-doehl@tuhh.de; anna.puestow@tuhh.de

Abstract **-** The alkali-silica reaction (ASR) is still a significant damage process in concrete structures. During an ASR poorly crystalline aggregate reacts with alkalis to form an alkali-silica gel. The alkali-silica gel causes damage by expansion within the concrete structure through the absorption of water. Since stopping an ASR is often not possible, costly and, time-consuming, preventive measures are taken and the use of reactive aggregates is avoided. Various test methods for the identification of alkali reactive aggregates already exist worldwide. However, there is currently no test method that can evaluate an aggregate in the short term without prior analysis, as in the case of an incoming goods inspection. In the Institute of Materials, Physics and Chemistry of Buildings at Hamburg University of Technology (TUHH) a new fast test method to identify alkali-reactive aggregates is being worked on. The test method is an accelerated dissolution experiment with ground aggregate like chemical testing methods, such as ASTM C289. But in the new approach, the reactivity of the aggregate is derived from the change in several chemical parameters due to a dissolution process. The dissolution process of the aggregate takes place in hot alkaline solution with an excess of alkalis. During the experiment, the pH-value, the electrical conductivity, and the redox potential are recorded as a function of time. Conspicuous points, such as extreme points and stationary states of these functions are to be used to evaluate the reactivity of the aggregate. It is assumed that the alkali reactivity of the aggregates is essentially reflected in the chemical parameters and thus, in reverse, a specific evaluation of the functions could provide indications of the reactivity of the aggregate. In this paper we present results regarding reaction kinetics and show possibilities to use this new method as an indicator for the reactivity of an aggregate.

Keywords**:** ASR, ASR testing method, electrical conductivity, durability, reaction kinetics

1. Introduction

1.1. The alkali-silica reaction

The alkali-silica reaction (ASR) is a reaction in the pore space of concrete whose reaction product is an expansive gel. The swelling gel leads to expansive strain, which damages the structure when reaching the tensile strain capacity of the concrete [1]. ASR does not occur in every concrete structure, although the three main constituents of concrete usually include the preconditions for an ASR. The alkali and hydroxide ions involved in an ASR are provided mostly by the cement and the required moisture is available due to the mixing water of the concrete. Since both preconditions can also reach the reaction site from the outside, it is practically impossible to completely prevent these two factors. However, the aggregate in the concrete has the greatest influence on whether ASR takes place. Only a lattice-disordered, amorphous, or even cryptocrystalline aggregate takes part in the reaction [1–3]. There is a distinction between fast-reacting and slow/late reacting aggregates. The first contain minerals such as opal and chalcedony, which in small quantities can cause damage within a few months, and the second contain, for example, strained or cryptocrystalline quartz. In this case it takes several years for a visible damage and a higher quantity of the reactive material is necessary [2, 3].

Since stopping an ASR is often not possible and complex once it has started, a preventive avoidance strategy is extremely important. The easiest and most reliable preventive measure to avoid it is the exclusion of aggregates with alkali-reactive minerals for the concrete [4–6]. There are different similar national testing methods to estimate the reactivity of an aggregate. The basic test methods are a petrographic investigation [6–8], methods based on reaction-dependent expansion of a standardized sample made of concrete or mortar [6, 9–11] and chemical testing methods [6, 12].

For the classification of an aggregate, only one test method is rarely sufficient. An allegedly reactive tested aggregate is usually retested using a different test method before it is finally classified as alkali reactive. The sequence of test methods

and adjustments are specified in the respective national standards. The length of time required to finally assess the material in terms of reactivity, the need for several different test procedures, standardized specimens and petrographic examinations of the material show that there remains a demand for optimization with regard to the identification of alkali-reactive aggregates. Furthermore, there is a lack of test procedures with which the alkali reactivity of the material can be determined in the short term.

1.2. Aims of this study

The objective of this research at Hamburg University of Technology (TUHH) is to develop a fast and reliable test method for categorizing any aggregate with respect to their alkali reactivity, without a prior classification of the aggregate, without a preparation of concrete or mortar specimen, and without elemental analyses or further chemical post-treatment. This test method is based on dissolution experiments, like in ASTM C289 [12]. The approach involves the reaction of ground aggregate in hot alkaline solution. During the dissolution, chemical and physical parameters are measured continuously, and changes in these parameters are intended to provide information about the alkali reactivity of the material. By using 1 M potassium hydroxide (KOH) as a solution, the aggregate is exposed to an alkaline environment like in the pore solution but with an oversupply of alkali hydroxides and water. Grinding the aggregate for enlarging the surface area and a constant experimental temperature of 60°C accelerate the dissolution process of the material. The parameters recorded are pH, redox potential, and electrical conductivity.

Initial tests have already been carried out with different aggregates of known alkali reactivity which were determined by the classical test procedures. It was found that the changes in chemical and physical parameters follow a certain regularity. In addition, mathematically quantifiable values such as extreme values and stationary points and their time of appearance can be determined. The exact size and time of these characteristic points are primarily influenced by the sample type, but also by the sample quantity. Thus, the courses of the three parameters can be differentiated in relation to the sample material. The aim of these investigations is to identify the influence of the alkali reactivity of the material on the time courses of the parameters and to derive limit values for the evaluation of further aggregates.

The recorded parameters are intended to visualize the various processes of aggregate dissolution. The electrical conductivity reflects the mobility and distribution of charged particles and the resistance of the solution. The pH was chosen since it shows the activity of hydroxide and hydroxonium ions in the solution, and the redox potential should show changes in the solution that do not affect either the pH or the electrical conductivity. This paper presents studies of the electrical conductivity of two flint stones with different but known alkali reactivity. A purely amorphous material is also presented as a reference. Investigations of pH and redox potential as well as other aggregates will be part of future contributions.

1.3. Electrical Conductivity and Reaction Mechanism

The electrical conductivity of a solution is anti-proportional to the resistivity of the solution and is the sum of the number of all charge carriers within the solution, whereby no distinction can be made between the individual ion types. The velocity, the mobility, and the charge of the considered ions enter into the conductivity, as well as the Faraday constant. The molar conductivity is a substance constant and independent of the concentration of the ion. However, above a certain concentration, the molar conductivity of the solution is no longer proportional to the concentration of the ion. If this concentration is exceeded, the conductivity of the solution decreases again as a function of the concentration. Interionic interactions are responsible for this reduction. The ions hinder each other in their mobility and velocity, the resistance of the solution increases and the conductivity decreases. Ion radii also have a reinforcing effect on the interionic interactions. A larger ionic radius reduces the conductivity of the solution. At vanishingly small concentrations, this relationship can be quantified using Kohlrausch's square root law. Thus only in infinite dilution are molar conductivities substance specific, in general they depend on the concentration of all ions in solution [13, 14].

The new test method imitates the reaction in the pore fluid of the concrete of the aggregate with highly alkaline solution. The contact between the reactive silicate aggregate and the alkaline solution triggers many different processes. On the one hand, these processes increase the number of charge carriers in the solution and thus also the conductivity. On the other hand, more and larger species are released into the solution, which increase the resistance of the solution

and thus decrease the conductivity. The conductivity recorded during the experiment is a sum parameter that merely shows the result of the opposing processes. However, here it is used to determine the reaction and rate constants of the sum of these reactions.

Generally, in alkaline solutions, such as the pore fluid, hydroxide ions first deprotonate the silanol groups (Si-OH) on on the surface of the silicate solid. This process decreases the concentration of hydroxide ions in the solution and leads to a predominantly negatively charged surface ($Si\text{-}O^-$) of the solid [15, 16]. The alkali cations of the solution counterbalance the negative surface of the silica solid. The resulting neutral surface can then be reached by the hydroxide ions, which attack the siloxane bonds of the solid. This releases silica into the solution by consuming hydroxide ions [16]. The silicates can be dissolved as mono-silicic acid (H_4SiO_4) or as oligomers ($Si_nO_a(OH)_b$ with $2a + b = 4n$) [15]. Mono-silicic acid is a weak acid with the ionization constants $K_1 = 10^{-9.8}$ and $K_2 = 10^{-12.4}$ [17]. Therefore, in highly alkaline solutions, such as the pore solution, the mono-silicic acid deprotonates to its anion $(SiO(OH)_3)^{-1}$ and its dianion $(SiO_2(OH)_2)^{2-}$, consuming hydroxide ions [17, 18]. Since the equilibrium concentration of the dissolved silicon depends on the amount of mono-silicic acid in the solution, the formation of the anions results in further solution of the solid [15]. Mono-silicic acid and its anions condensate to polysilicic acids [19, 20]. The dissolution rates for crystalline and amorphous silica lead to the assumption that they follow the same reaction pathway, though the dissolution rate of amorphous silica is higher [21]. A lower silica concentration in the solution also leads to slower polymerization of the mono-acid [1].

The new test method utilizes the different dissolution and condensation behaviour of the individual aggregate, which is affected by their alkali reactivity and can be shown in the reaction rate of the electrical conductivity.

2. Methods and Material

2.1 Experimental setup

The new test method was first mentioned and precisely described in Osterhus and Schmidt-Döhl [22]. The experimental setup, seen in Figure 1 consists of a test container (8) made of Polytetrafluoroethylene (PTFE) where reaction kinetics and chemical parameters are directly measured with electrodes (1-4). To keep the contact between the KOH solution in the container and air to a minimum the container is closable hermetically, and the aggregate is added throw a small inlet which is closed with a PTFE screw (7). Sedimentation of the aggregate is prevented by a magnetic stirrer (5, 6) located at the bottom of the PTFE container. During this experiment, the whole container is heated in a bath with a circulation thermostat (11). Before every experiment all electrodes are calibrated. The 1 M potassium hydroxide solution is made by mixing 56.11 g KOH-platelets with 1 l of distilled water and the previous grind aggregate is weighed to the nearest 0.001 g and stored for 24 hours in an oven at 60°C. With reaching constant initial conditions of all the measured parameters, the aggregate is added and after 48 hours, the experiment is terminated.

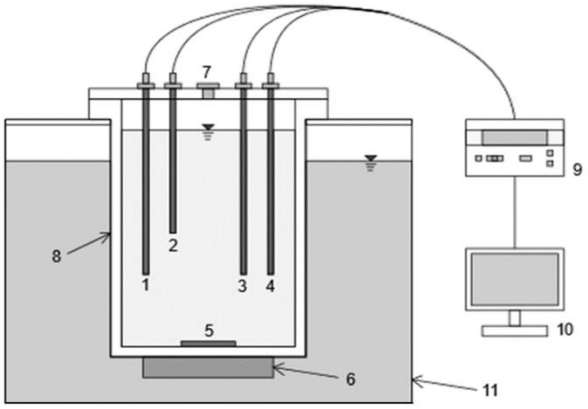

Figure 1: experimental setup with: (1) pH electrode, (2) temperature sensor, (3) electrical conductivity electrode, (4) redoxpotential electrode, (5) agitator, (6) magnetic stirrer, (7) opening for sample addition, (8) experimental reactor, (9) multiparameter device, (10) computer, (11) heat bath

The pH-value, the redox potential, the temperature, and the electrical conductivity are taken every 30 seconds. The time of adding the aggregate is set as point zero for all measurements. Characteristic points such as steady states and minima are identified with Microsoft excel.

Previous research in literature only describes dissolution experiments with silicate aggregate either at much higher temperatures, in lower pH-values, or with a different ratio of dissolving hydroxide ions to soluble silicate aggregate. The specific approach of exposing a rigidly ground aggregate to an excess of alkalis in a highly alkaline solution at a temperature of 60°C and then measuring the three parameters mentioned here has not yet been attempted to date. Therefore, there are no comparative values in the literature regarding the change of the parameters so far.

2.2 Material

The chemical composition of the aggregates was determined by XRF spectroscopy with the RFA Horiba XGT-7200 spectrometer. Results were analysed using the fundamental parameter method and the "NIST1881s" reference standard. The specific surface was determined according to BET with N_2-sorption using a Micromeritics Accelerated Surface Area and Porosimetry System 2010 (ASAAP 2010). The particle size distribution was measured with a laser diffraction system (Mastersizer 3000 by "Malvern"). Reference data of an inert aggregate was generated with quartz powder (QP) from "MILLISIL" [23] by Osterhus and Schmidt-Döhl [22, 24]. All electrodes used are from "Xylem Analytics Germany Sales GmbH & Co. KG" and specially selected for the highly alkaline conditions and high temperatures. The pH electrodes show no alkali error.

The investigated aggregates in this contribution are microsilika (MS) and two different flintstones. Quartz powder was used to compare the results with a non-reactive material. The two different flints (F_AD, F_NB) were characterized, and their alkali reactivity was determined by density according to the German alkali guideline [6]. The density of F_AD is 2.41 g/cm^3 and F_NB has a density of 2.59 g/m^3. The reactive parts were calculated according to [6] with the result that F_AD contains 26.75% reactive structures and F_NB 1.75%. Consequently, F_AD is considered reactive in the sense of an ASR and F_NB is considered harmless.

The results of the chemical and physical properties of the flintstones are summarized in Table 1. SiO_2 is the main component and there are just traces of CaO, Fe_2O_3 and K_2O in both aggregates. The specific surface of both is similar and ranges between 3.64 and 7.88 m^2/g. According to the manufacturer, microsilica has a specific surface of 15 m^2/g, a silicate content of at least 85% and an average particle size of 0.1 μm. The numbers of the experiments which are the basis for this paper's investigations for F_AD, F_NB, microslica and the quartz powder, are also listed in Table 1. The sample quantities vary between 3 g and 12 g. Thus, an oversupply of potassium hydroxide is guaranteed, and a sufficient amount of aggregate is available to cause significant changes in the measurement parameters.

Table 1: Characterization of the siliceous materials

	BET	True Density	D_{10}	D_{50}	D_{90}	SiO_2	Numbers of experiments				
	[m^2/g]	[g/cm^3]	[µm]	[µm]	[µm]	[%]	3g	5g	8g	10g	12g
F_AD	7.88	2.41	0.7	2.62	15.2	98	4	6	4	5	4
F_NB	3.64	2.59	1.03	3.11	11.84	98.5	10	5	8	6	4
MS	15	2.16	-	0.1	-	85 - 98	3	7	3	8	-
QP	0.9	2.65	10.0	16.00	42.86	99	-	-	-	4	-

3. Results and discussion

The electric conductivity is dividable into three different sections, as seen in Figure 2. In the first section, section A, only the hot KOH is measured, resulting in a constant value LF_0. After adding the aggregate section B starts. The electrical conductivity decreases until it reaches a constant value, LF_1 again in section C. Addition of the non-reactive quartz flour, however, does not lead to any change in conductivity.

For a better comparison of the results among each other, the data was normalized by LF_0. This sets the conductivity in section A to 1. This normalization also shows immediately the amount of reduction of the conductivity. LF_1 is thus the percentage reduction in conductivity after the addition of the sample. The normalized time courses of a sample type and quantity accumulate with only slight deviation, as can be seen in Figure 3 for microsilica. In addition, a sorting with respect to the sample quantity can be seen. The conductivity decreases more in experiments with larger sample quantities. In order to better understand the opposing reactions of the dissolution process, to determine and quantify differences in the reactions as a function of the sample type and quantity and the influence of the reactivity of the aggregate, functional equations are determined for the normalized conductivity curves.

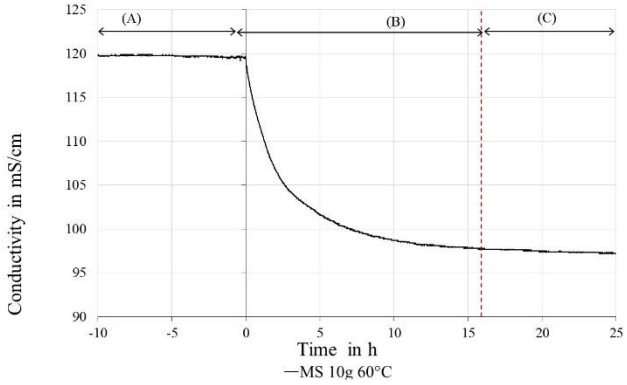

Figure 2: The electrical conductivity in general and divided in sections.

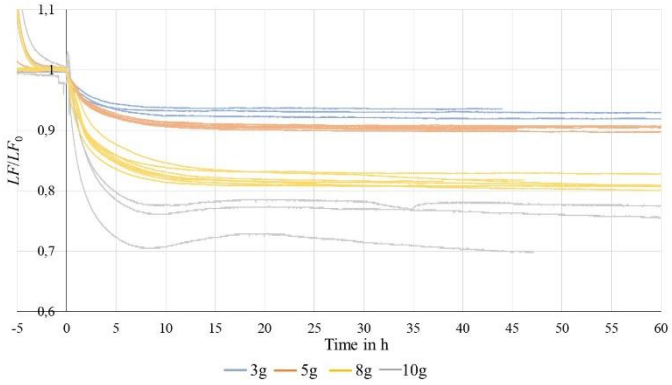

Figure 3: The electrical conductivity sorted by sample amount.

Initially, a first-order reaction is assumed. However, both the processes that increase conductivity and those that decrease conductivity are to be considered. This is not given in the simplest form of a first order reaction. Therefore, conductivity is modelled from two different functions. One gives the increase in conductivity and the other the decrease. These two functions are based on decay and growth functions and thus represent first order reactions. The increase in conductivity due to more charge carriers in the solution is represented by a growth function $IC_{\mathrm{LF}}(t)$, see Eqs. (2). The increase of the resistance of the solution and thus the reciprocal decrease of the conductivity by a decay function $DC_{\mathrm{LF}}(t)$, Eqs (1). The sum of both functions, $LF_{\mathrm{m}}(t)$, then shows the summed change in the charge carriers of the solution and hence the variation in electrical conductivity, as seen in equations Eqs. (3).

$$DC_{\mathrm{LF}}(t) = g_{\mathrm{dc}} + d_{\mathrm{dc}} \times \mathrm{e}^{-k_{\mathrm{dc}} \times t} \tag{1}$$

$$IC_{\mathrm{LF}}(t) = g_{\mathrm{ic}} + d_{\mathrm{ic}} \times \mathrm{e}^{-k_{\mathrm{ic}} \times t} \tag{2}$$

$$LF_{\mathrm{m}}(t) = DC_{\mathrm{LF}}(t) + IC_{\mathrm{LF}}(t) = g_{\mathrm{ic}} + g_{\mathrm{dc}} + d_{\mathrm{ic}} \times \mathrm{e}^{-k_{\mathrm{ic}} \times t} + d_{\mathrm{dc}} \times \mathrm{e}^{-k_{\mathrm{dc}} \times t} \tag{3}$$

Where t is the time as a running variable, g_{ic} and g_{dc} are the respective limit values of the function when t tends to infinity and, k_i are the rate constants. Furthermore, $d_i = s_{\mathrm{i}} - g_{\mathrm{i}}$, whereby s_{i} is the value of the function for $t = 0$. For $DC_{\mathrm{LF}}(t)$, $d_{\mathrm{dc}} > 0$, meaning that the function value for $t = 0$, s_{dc} is greater than the limit value of the function, g_{dc} and in the case of $IC_{\mathrm{LF}}(t)$, $d_{\mathrm{ic}} < 0$. The following assumptions were made to determine the unknowns in the model functions. The function $LF_{\mathrm{m}}(t)$ reaches the limit LF_1 when t approaches infinity and $LF_{\mathrm{m}}(0) = LF_0$ is valid. Accordingly, the limit values of the functions $DC_{\mathrm{LF}}(t)$, g_{dc} and $IC_{\mathrm{LF}}(t)$, g_{ic} complement each other to LF_1 and $LF_1 = g_{\mathrm{dc}} + g_{\mathrm{ic}}$ holds. Furthermore, the sum of the initial values of the functions DC_{LF}, s_{dc} and IC_{LF}, s_{ic} results in the initial value of $LF_{\mathrm{m}}(0) = LF_0$. Thus, $LF_0 = s_{\mathrm{dc}} + s_{\mathrm{ic}}$ is valid. The rate constants are determined from the experimental data. For this purpose, following the classical half-life, the value between LF_0 and LF_1 with $LF_{0.5} = LF_0 + 0.5LF_1$ and its point in time are determined. Since the experimental results do not allow a differentiation into the individual functions and the summed total function $LF_{\mathrm{m}}(t)$ is assumed, a common velocity constant k_{m} is also assumed initially and $k_{\mathrm{dc}} = k_{\mathrm{ic}} = k_{\mathrm{m}}$ therefore applies. These boundary conditions lead to the following equation (4) for $LF_{\mathrm{m}}(t)$.

$$LF_{\mathrm{m}}(t) = LF_1 + (LF_0 - LF_0) \times \mathrm{e}^{-k_{\mathrm{m}} \times t} \tag{4}$$

The model functions determined in this way reproduce the experimental results well, as can be seen for microsilica Figure 4. However, a deviation in the first minutes after sample addition is noticeable. The experimental data increase sharply for a short time directly after sample addition, which is not shown in the sum function $LF_{\mathrm{m}}(t)$ and argues for a differentiation of $LF_{\mathrm{m}}(t)$ into two subfunctions with different rate constants. However, the relevance of the differentiation seems to be less for advanced time, because with proceeding time the experimental data are reliably represented by $LF_{\mathrm{m}}(t)$.

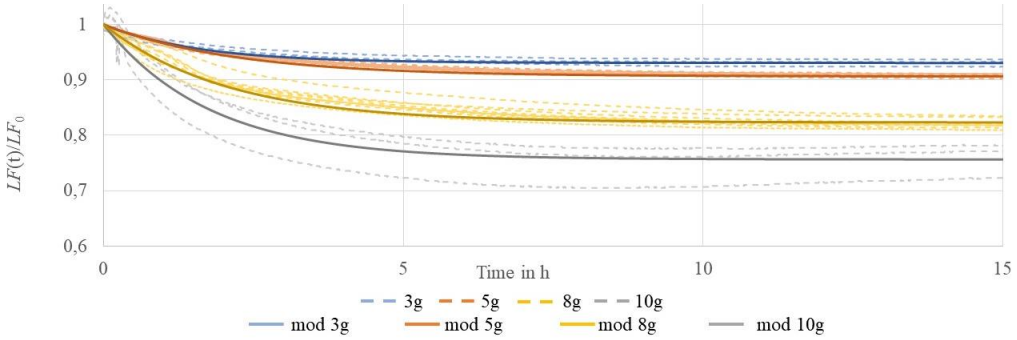

Figure 4: Experimental data of electrical conductivity and modulated functions for microsilica.

In a closer look at the reaction rate and equilibrium state LF_1 a sorting can be seen with respect to the reactivity of the materials in Figure 5. The non-reactive flint, FL_NB has smaller reaction rate, despite similar equilibrium LF_1, than the reactive flint FL_AD and significantly lower than microsilica. Moreover, in the case of flint, a decrease in reaction rate with larger LF_1 is seen. Thus, a greater reaction rate is accompanied by a more significant decrease in electrical conductivity. Except for one point, this tendency can also be observed with microsilica. Accordingly, the more reactive material adds to the solution not only faster but also a larger amount of interfering particles.

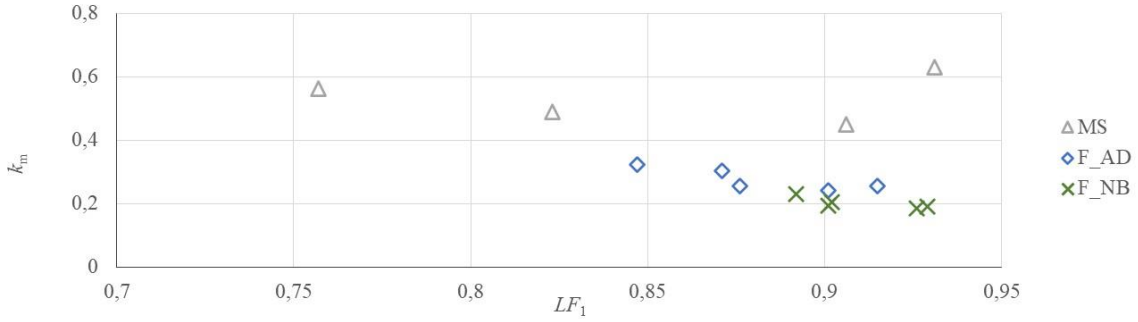

Figure 5: Reaction velocity k_{m} to the limiting conductivity LF_1

The rate constants of the individual functions should be proportional to the reactive surface of the aggregate. Figure 6 shows the rate constant to the reactive surface of the sample material. Despite more available surface area in solution, the rate constant increases only slightly and even tends to decrease for microsilica. When considering the rate constants normalized to the reactive surface area, it can be clearly seen that more reactive surface area leads to a decrease in the rate constant with respect to a square meter, as seen in Figure 7. Thus, the overall reaction per se becomes slower with more reactive surface. Again, a sorting with respect to reactivity can be seen. The non-reactive flint shows the lowest reaction rates even normalized with the reactive surface, and the purely amorphous microsilica shows the highest

reaction rates with similar surface area. The lack of proportionality of the rate constant to the surface area may be due to a perceived incorrect equation of the rate constants of IC_{LF} and DC_{LF} or to the assumption that the total reactive surface area contributes to the reaction.

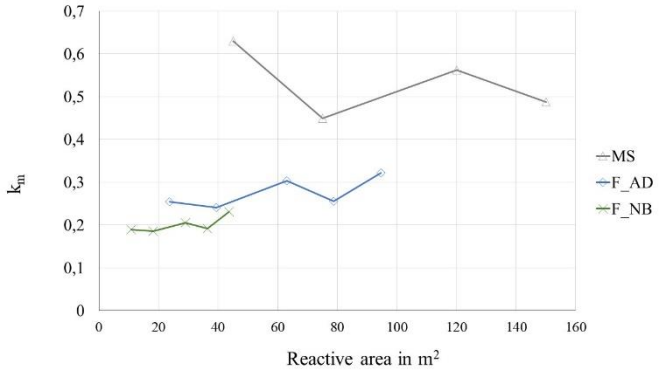

Figure 6: Reactive surface to reaction rate of reaction of all aggregates

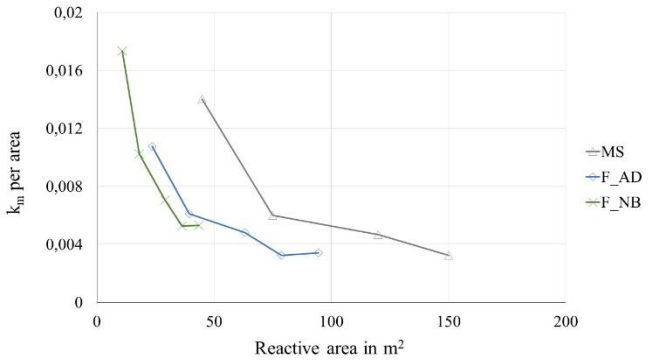

Figure 7: Reaction rate as a reaction of reactive area of all aggregates

4. Conclusion

To develop a new rapid test method for the identification of reactive aggregates, dissolution tests were carried out with ground aggregate in a potassium hydroxide solution at 60°C. During the dissolution process, the pH, conductivity, and redox potential are recorded. In this paper, results of electrical conductivity were discussed. The time course of the conductivity was modelled as a function of the sample quantity for two differently reactive flint and purely amorphous, that is, reactive microsilica. For this purpose, a first-order reaction was initially assumed. In addition, it was also assumed that processes take place during the dissolution experiment which have an opposite effect on the electrical conductivity. This was considered by summing two functions, one based on a growth function and the other on a decay function. The reaction rate was determined from the experimental data. Since this represents the sum of all reactions taking place, the reaction rate k_m of the total function LF_m was set equal to the reaction rates of the two individual functions. The modelled functions showed good results. A more detailed investigation of the reaction rate showed that it is not, as expected, proportional to the specific surface area. It can be concluded that either different reaction rates have to be considered in the overall equation or not all of the specific surface area contributes to the reaction. Nonetheless, a differentiation of the reaction rates with respect to the reactivity of the aggregate is possible. The reaction rate increases with increasing reactivity of the material and the rate constant normalized to the surface is larger in the case of the more reactive material compared to the less reactive aggregate.

Acknowledgments

The authors greatly acknowledges the funding of this research by the German Research Foundation (Deutsche Forschungsgemeinschaft, DFG) in the framework of Research Training Group GRK 2462: Processes in natural and technical Particle-Fluid-Systems (PintPFS) (390794421) [25] at Hamburg University of Technology.

References

[1] Z. Amjad, Ed. *Mineral scales in biological and industrial systems*. Boca Raton, Fla.: CRC Press, 2014.

[2] M. D. A. Thomas, B. Fournier, and K. J. Folliard *Alkali-aggregate Reactivity (AAR) Facts Book*: Federal Highway Administration, Office of Pavement Technology, 2013.

[3] I. Fernandes and M. A. T. M. Broekmans, "Alkali–Silica Reactions: An Overview. Part I," *Metallogr. Microstruct. Anal.* vol. 2, no. 4, pp. 257–267, 2013, doi: 10.1007/s13632-013-0085-5.

[4] P. J. Nixon and I. Sims, Eds. *RILEM Recommendations for the Prevention of Damage by Alkali-Aggregate Reactions in New Concrete Structures: State-of-the-Art Report of the RILEM Technical Committee 219-ACS*. Dordrecht: Springer Netherlands, 2016.

[5] ASTM C1778-20 *Guide for Reducing the Risk of Deleterious Alkali-Aggregate Reaction in Concrete*, 2020, West Conshohocken, PA.
[6] DAfStb *DAfStb-Richtlinie Vorbeugende Maßnahmen gegen schädigende Alkalireaktion im Beton: (Alkali-Richtlinie)*, 2013, Berlin.
[7] RILEM Recommended Test Method, AAR-1 *Detection of potential alkali-reacticity aggregates: Petrographic method*, 2003, RILEM TC 191-ARP.
[8] ASTM C295 *Guide for Petrographic Examination of Aggregates for Concrete*, 2019, West Conshohocken, PA.
[9] RILEM Recommended Test Method, AAR-2 *Detection of Potential Alkali-Reactivity of Aggregates: Accelerated Mortar-Bar*, 2003, RILEM TC 191-ARP.
[10] ASTM *C1260-21 Test Method for Potential Alkali Reactivity of Aggregates (Mortar-Bar Method)*, West Conshohocken, PA, 2021. [Online]. Available: www.astm.org
[11] ASTM C1293-20a *Test Method for Determination of Length Change of Concrete Due to Alkali-Silica Reaction*, 2020, West Conshohocken, PA.
[12] ASTM C289-07 *Standard test method for potential alkali-silica reactivity of aggregates (chemical method)*, 2007, West Conshohocken, PA.
[13] C. Czeslik, H. Seemann, and R. Winter *Basiswissen physikalische Chemie*, 4th ed. Wiesbaden: Vieweg + Teubner, 2010.
[14] G. Wedler *Lehrbuch der physikalischen Chemie*, 5th ed. Weinheim: Wiley-VCH, 2010.
[15] F. Rajabipour, E. Giannini, C. Dunant, J. H. Ideker, and M. D. Thomas, "Alkali–silica reaction: Current understanding of the reaction mechanisms and the knowledge gaps," *Cement and Concrete Research* vol. 76, pp. 130–146, 2015, doi: 10.1016/j.cemconres.2015.05.024.
[16] D. Bulteel, E. Garcia-Diaz, C. Vernet, and H. Zanni, "Alkali–silica reaction," *Cement and Concrete Research* vol. 32, no. 8, pp. 1199–1206, 2002, doi: 10.1016/S0008-8846(02)00759-7.
[17] J. Eikenberg, "On the Problem of Silica Solubility at High PH," *PSI*, no. 74, p. 57, 1990.
[18] J. H. M. Visser, "Fundamentals of alkali-silica gel formation and swelling: Condensation under influence of dissolved salts," *Cement and Concrete Research* vol. 105, pp. 18–30, 2018, doi: 10.1016/j.cemconres.2017.11.006.
[19] K. Goto, "Effect of pH on Polymerization of Silicic Acid," *J. Phys. Chem.* vol. 60, no. 7, pp. 1007–1008, 1956, doi: 10.1021/j150541a046.
[20] S. A. Greenberg, "The Depolymerization of Silica in Sodium Hydroxide Solutions," *J. Phys. Chem.* vol. 61, no. 7, pp. 960–965, 1957, doi: 10.1021/j150553a027.
[21] P. M. Dove, N. Han, A. F. Wallace, and J. J. de Yoreo, "Kinetics of amorphous silica dissolution and the paradox of the silica polymorphs," *Proceedings of the National Academy of Sciences of the United States of America* vol. 105, no. 29, pp. 9903–9908, 2008, doi: 10.1073/pnas.0803798105.
[22] L. Osterhus and F. Schmidt-Döhl, "Verbessertes Prüfverfahren zur Beurteilung der Alkalireaktivität von Gesteinskörnungen basierend auf Lösungsversuchen," in *GDCh-Monographie Band 48: Tagung Bauchemie 2014*, 2014, S. 41-44.
[23] Quarzwerke *Datasheet MILLISIL-Mehle.* Accessed: Apr. 28 2021. [Online]. Available: https://www.quarzwerke.com/fileadmin/quarzwerke/Leistungserklaerungen/Leistungserkl-Sortenverz-EN12620-SMF_Revision_1.pdf
[24] L. Osterhus, C. Dombrowski, and F. Schmidt-Döhl, "Löslichkeitsuntersuchungen zur schnellen Beurteilung der Alkalireaktivität von Gesteinskörnungen," *19. Int. Baustofftagung ibausil*, 16 Sep., pp. 1405–1412, 2015.
[25] DFG Research Training Group *GRK 2462 processes in natural and technical Particle-Fluid-Systems (PintPFS).* [Online]. Available: https://gepris.dfg.de/gepris/projekt/390794421 (accessed: Dec. 12 2022).